Carbon monoxide dissociation at planetary entry conditions examined by MHz-rate laser spectroscopy

Nicolas Minesi, Lok Lai, Miles Richmond, Christopher Jelloian, R. Mitchell Spearrin

Carbon monoxide dissociation at planetary entry conditions examined by MHz-rate laser spectroscopy

Nicolas Q. Minesi*†, Lok H. Lai‡, Miles O. Richmond§, Christopher C. Jelloian¶, and R. Mitchell Spearrin‖
University of California, Los Angeles (UCLA), Los Angeles, California 90095

A study of carbon monoxide (CO) dissociation was performed in a shock tube at conditions relevant to high-speed entry of Venus and Mars atmospheres. The CO number density (or mole fraction) and the temperature are probed behind reflected shock waves at 1 MHz using scanned-wavelength laser absorption spectroscopy near 2011 cm^{-1} (4.97 µm). The wide range of vibrational states (v" = 1, 4, 8, and 10) probed by this technique enables precise number density and temperature measurements up to and above 9000 K using a Boltzmann population fit of the resolved spectral lines. Mixtures of CO diluted in Ar at 3% – 60% are shock-heated in a wide range of conditions (T_5 = 4,650 – 11,150 K at p_5 = 0.26 – 4.07 atm) and compared to state-of-the-art chemical kinetic models. The time-resolved measurements of temperature and number density behind reflected shock waves are utilized to infer the rate coefficients of CO + M → C + O + M for M = CO, Ar. They are found to be $k_{\text{diss, CO}} = 1.8 \times 10^{28} \cdot T^{-2.7} \exp(-129,000/T)$ cm^3/(mol·s) and $k_{\text{diss, Ar}} = 1.5 \times 10^{25} \cdot T^{-2.1} \exp(-129,000/T)$ cm^3/(mol·s).

I. Introduction

Convective and radiative heating on an entry vehicle is particularly sensitive to the atmosphere's thermochemical state. During Mars and Venus entry, a significant fraction of the mixture is composed of carbon monoxide, CO, which is the major radiation source for speeds above 6 km/s [1]. CO can also be formed in any atmosphere due to the sublimation and oxidation of the surface material of a hypersonic vehicle [2, 3]. Despite the critical importance of CO formation and depletion in such environments, there is still uncertainty regarding its non-equilibrium kinetics, especially dissociation. CO dissociation has long been studied using optical diagnostics in shock tubes, but the rate coefficients found by different groups span across several orders of magnitude. In 1994, Park et al. [4] proposed a kinetic mechanism and an elegant solution to simulate vibrational and electronic non-equilibrium. This well-established model has been shown to be sufficient to describe the radiation occurring in Mars entry at < 6.6 km/s but was found to be

*Post-doctoral scholar, Mechanical and Aerospace Engineering Department, AIAA Member
†Current affiliation: Assistant Professor, EM2C, CentraleSupélec, Université Paris-Saclay (France), nicolas.minesi[at]centralesupelec.fr
‡Graduate student, Mechanical and Aerospace Engineering Department
§Graduate student, Mechanical and Aerospace Engineering Department
¶Ph.D., Mechanical and Aerospace Engineering Department, AIAA Member
‖Associate Professor, Mechanical and Aerospace Engineering Department, AIAA Member
Presented as Paper 2023-3731 at the AIAA Aviation Forum, 12-16 June, 2023 in San Diego, CA

erroneous at higher speeds [5, 6]. This discrepancy has renewed interest in Mars and Venus kinetics during entry and the improvement of the CO dissociation rate, which is important in prediction of the thermo-chemical state at high entry velocities [6, 7].

Dissociation of CO becomes significant above 5,000 K, which motivates the development of diagnostics to measure its spatiotemporal evolutions near this temperature and higher. A number of optical techniques have been utilized previously for CO sensing at entry temperatures including optical emissions spectroscopy (OES) and broadband absorption in a steady-state plasma torch [2] as well as laser absorption spectroscopy (LAS) in shock tubes [7–13]. As high entry velocities yield shock-induced temperatures approaching 10,000 K, the characteristic kinetic time is near the µs scale. Unfortunately, many of the previously-developed diagnostics are not well-suited to achieve this time resolution or temperature range. Single-line scanned LAS with µs-resolution was developed in [7–10] where the temperature (2,500 – 10,000 K) was measured relying on Doppler broadening of a CO transition in the infrared (IR). This strategy is however limited to low-pressure environments where Doppler broadening is the dominating broadening mechanism. A more recent study from our group has demonstrated measurements at MHz rates of CO mole fraction and temperature via multi-line laser absorption sensing and Boltzmann regression [14]. The present work leverages this novel experimental development to perform a kinetic study of CO dissociation across a wide range of temperatures in a high-enthalpy shock tube.

This paper describes the experimental approach and resulting dataset used to infer CO dissociation rates over a range of conditions relevant to planetary entry. In Section II, the experimental setup and the measurement technique of our previous study [14] are quickly described for context. In Section III, the rate optimization procedure is presented to reconcile simulated and measured species and temperature time histories. Finally, in Section IV, the results of the rate inference are presented and discussed in the context of a review of the available rates in the literature.

II. Experimental setup and spectroscopy methods

The shock tube experimental setup and the methods for fitting and interpreting the CO absorption lines are described in our previous work [14] and are summarized here. The UCLA high-enthalpy shock tube (HEST), fully described in [15, 16], is presented in Fig. 1. A 1.5-m driver section is filled with helium until a plastic or metal diaphragm bursts and generates a shock wave in the 4.9-m driven section. Mixtures of CO diluted in argon are manometrically prepared in a stirred mixing tank. The concentration of CO ranges from 3% to 60%. The tank is vacuumed down to less than 20 mTorr before preparing the mixtures. The purity of CO and Ar gases is certified above or equal to 99.99% by Airgas. The combined pressure and pure gas uncertainties result in a relative mixture composition uncertainty always below 0.05%. Thus, the uncertainty of the reference mixture is assumed to be negligible.

The optical setup is schematically presented in Fig. 1. The mean current and temperature of a quantum cascade laser (Alpes Lasers) are regulated using a laser controller (Arroyo 6310). A fixed (DC) current is sent to the laser via

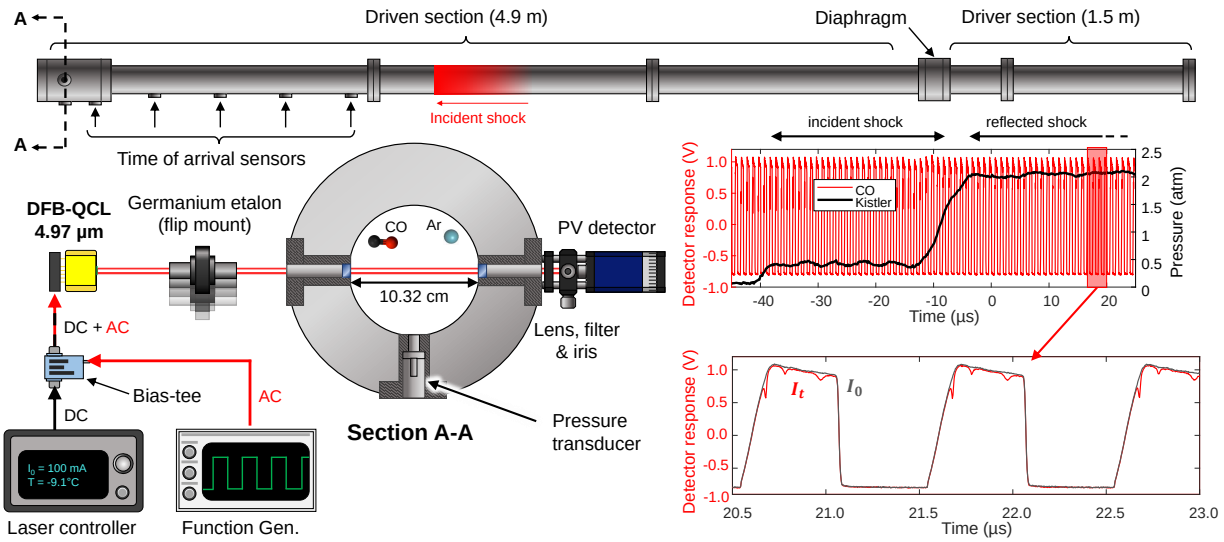

Fig. 1 (Left) Optical alignment setup mounted on the UCLA high-enthalpy shock tube (HEST). (Right) Sample raw detector and pressure measurements. In the inset, the time-resolved measurements (in red) are compared with the averaged background (in dark grey). Reprinted with permission from [14].

the controller, while a 1-MHz voltage modulation (or RF signal) is diplexed to this DC component with a bias-tee circuit [17]. In this work, the laser is modulated with a trapezoidal waveform in order to maximize signal-to-noise ratio and scan depth while not exceeding the bandwidth limitations of the detection system [18]. The current amplitude is set to 80% of the maximum allowed by the laser manufacturer. This setting represents a compromise between hardware safety and spectral scan depth, reaching 1 cm^{-1}. The trapezoidal waveform, shown in Fig. 1, presents a ramp on the increasing side. This ramp prevents the temporal frequency content of the raw electrical signal from being higher than the limiting bandwidth of the detection system (200 MHz) when narrow absorption features are present in the scan. Following the recommendations of [18], we ensured that the equivalent time to scan an FWHM of the CO line is greater than 10 ns (twice the inverse of 200 MHz) to prevent instrument broadening resulting in spectral distortion.

A Voigt lineshape fitting routine and a Boltzmann regression are employed to recover absorption areas of the targeted transitions and infer gas properties. Four CO transitions – R(8,24), R(10,115), P(4,7), and P(1,25) – are scanned at 1 MHz across 2010.6–2011.6 cm^{-1}, see Fig. 2. The CO linestrengths and CO partition function are calculated using the HITEMP 2019 database [19, 20]. Using the areas of these lines, a Boltzmann population fit is performed and provides CO number density and temperature. The fitting procedure is performed assuming equilibrium of the rotational and vibrational temperatures, which is expected in the conditions explored here. Uncertainties in the data processing are calculated according to the methods in [14, 17]. The 1-MHz sampling being extremely fast compared to the timescale of temperature and CO mole fraction evolution, the raw data are processed with a 1-µs resolution but are time-averaged at select conditions. This procedure improved the signal-to-noise ratio of the experimental spectra, which in turn reduced the uncertainty (scaling with the square root of the number of measurements in the average). Thus, the uncertainty is

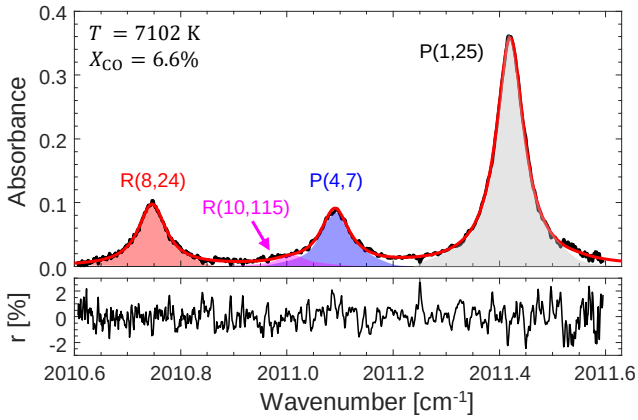

Fig. 2 Typical fit of the CO absorption spectrum between 2010.6 and 2011.6 cm^{-1}. Reprinted with permission from [14].

typically within 3–5% for number density and 1–3% for temperature.

III. Kinetic rate analysis

A. Methodology

This section describes the chemical kinetic rate analysis and the procedure for inferring rate coefficients from the laser spectroscopy dataset. A full review of the available rate coefficients is provided in Section IV. The kinetic mechanism of Johnston and Brandis [6] was employed to run the sensitivity analysis and perform the rate optimization. For the present case in a CO and Ar mixture, the Johnston and Brandis mechanism is equivalent to the mechanism of Park et al. [4] with an adjustment of the C_2 and CO dissociation rate coefficient. Note finally that this mechanism was recommended at high temperatures by Cruden et al. [7]. It is denoted here as the "baseline mechanism". The baseline mechanism with the modified rate coefficients is denoted the "modified mechanism". Both mechanisms are provided as supplementary material. In the modified mechanism, only the rate coefficients of (R1) and (R2) are altered from the baseline mechanism.

$$\mathrm{CO + CO \longleftrightarrow C + O + CO} \tag{R1}$$

$$\mathrm{CO + Ar \longleftrightarrow C + O + Ar} \tag{R2}$$

A Cantera 0-D constant-pressure reactor model is used to simulate the shock-heated gas. The reactor pressure is updated in the simulation time loop according to an isentropic compression law to account for the slight pressure increase measured by the piezoelectric sensor (typically a few mbar / 100 µs). The temperature increase due to a positive (dp/dt) was already included in data correction and 0D kinetic simulations before, see [21]. Therefore, the reactor temperature is updated accounting for the kinetics of CO dissociation (mostly endothermic) and the aforementioned isentropic compression. The model does not account for the effect of a boundary layer. The thermodynamic coefficients

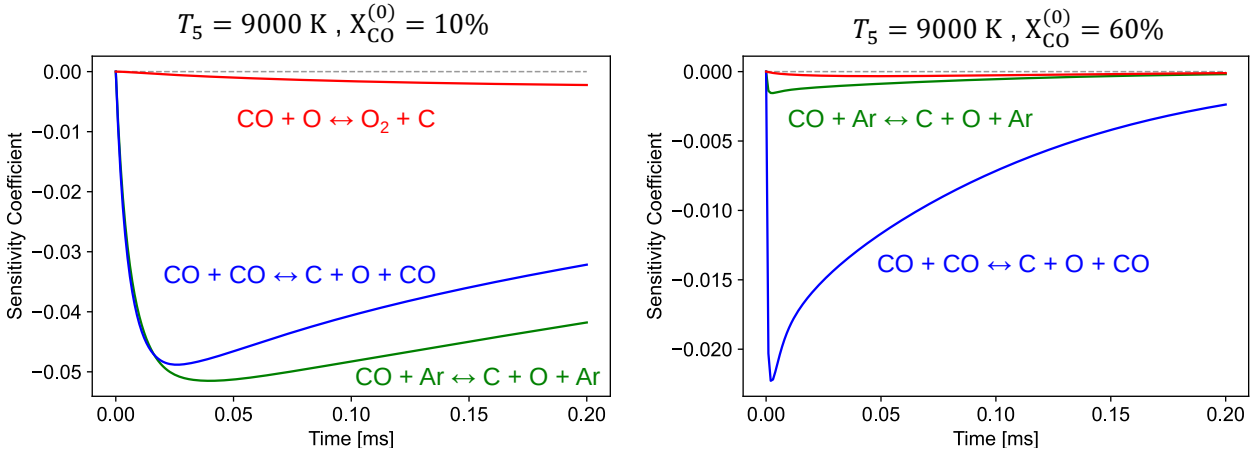

Fig. 3 Sensitivity analysis of CO mole fraction using the baseline mechanism. The simulations are run in a mixture shock-heated at 9000 K and 1 atm where the temperature is allowed to vary due to the endothermic dissociation reactions. The sensitivities are calculated for two mixtures: (left) CO:Ar = 10:90 and (right) CO:Ar = 60:40.

are taken from the NASA9 thermodynamic database [22], which is valid up to 20,000 K. The values of these coefficients are available in the supplementary materials (.YAML files).

In this work, all temperatures (translational, rotational, and vibrational) are assumed to be equal. The vibrational-translational (VT) relaxation time after the normal reflected shock can be estimated using the empirical relation of Millikan and White [23] with the values of Park [4]. In the experimental conditions employed in this work (T_5 = 4,650 – 11,150 K at p_5 = 0.26 – 4.07 atm), the VT relaxation time is equal or below 4 µs and always below 2 µs above 8000 K. This delay has no impact on our rate determination because the first few microseconds after the normal shock were systematically removed in the fitting procedure to neglect the impact of a potential shock bifurcation.

The presence of electronically excited states is neglected (see [24], for instance, for a more refined model). In the following, the key reaction rates are identified by sensitivity analysis and an optimization procedure is employed to infer the values of these rates over a range of test conditions.

B. Sensitivity analysis

A sensitivity analysis of reactions with respect to CO mole fraction is conducted and shows that two reactions are largely dominating CO dissociation: (R1) and (R2). In Fig. 3, the relative impact of the two reactions is shown for a simulated shock at P_5 = 1 atm and T_5 = 9000 K. Note that these initial temperatures evolve with time as the endothermic dissociation of CO progresses. As could be predicted for a highly diluted CO mixture, CO dissociation is driven by CO-Ar collisions (R2). However, in a mixture of CO:Ar = 60:40, the rate coefficient of CO-CO collisions (R1) is one order of magnitude higher than that of (R2). Therefore, with the experiments performed in this study ranging from 3 to 60% CO dilution, both rate coefficients of (R1) and (R2) are important and can be tuned.

As discussed later in Section IV.B, some work has suggested that the impact of atomic oxygen exchange could be important [25–27]. In that case, CO dissociation would be driven by the following two-step mechanism:

$$CO + O \longleftrightarrow O_2 + C \tag{R3}$$

$$O_2 + M \longleftrightarrow O + O + M \tag{R4}$$

As demonstrated Fig. 3, the sensitivity of CO mole fraction to (R3) is typically one order of magnitude below that of (R1) or (R2). Note that the sensitivity of CO mole fraction to (R3) and (R4) is the same. This conclusion is in line with the work of Cruden et al. [7], who demonstrated via fundamental principles that CO dissociation is not driven by O atom exchange, even in undiluted (pure) CO. Thus, for the rest of this work, the rate coefficients of (R3) and (R4) will remain unchanged.

Finally, the conclusions of this analysis depend on the set of rate coefficients employed in the sensitivity computation. As shown in Section IV, our proposed rate coefficients of (R1) and (R2) are higher than those proposed in the baseline mechanism of Johnston and Brandis. Consequently, the influence of reactions (R3) and (R4) on the CO mole fraction would be further reduced using the modified mechanism.

C. Optimization

A range of shock tube experiments producing initial reflected shock conditions from T_5 = 4,650 to 11,150 K was completed, yielding species and temperature time histories that could be compared to the baseline mechanism. During test times on the order of 100 µs, CO dissociation was noticed above 5000 K via the temperature data. In Fig. 4 from top to bottom, the measured CO number density, $N_{CO}[\mathrm{cm}^{-3}]$, the CO mole fraction, X_{CO}, and temperature, $T[\mathrm{K}]$ are compared to simulated values. Experimentally, N_{CO} and T are calculated from the transition areas in the CO spectrum with full details on the measurement procedure provided in [14], see Section II. The mole fraction is calculated from Eq. 1, where $P[\mathrm{Pa}]$ is the pressure and $k_B = 1.38 \times 10^{-23}$ [J/K] is the Boltzmann constant.

$$X_{CO} = \frac{N_{CO}}{P/k_B T} \tag{1}$$

In this work, the pressure is calculated in Eq. 2 from the pressure predicted by normal shock relations, P_5, and accounting for a slight linear increase of pressure measured by the pressure transducer on the shock tube wall, dp/dt, multiplied by the time after the reflected shock, t:

$$P = P_5 + (dp/dt) \times t \tag{2}$$

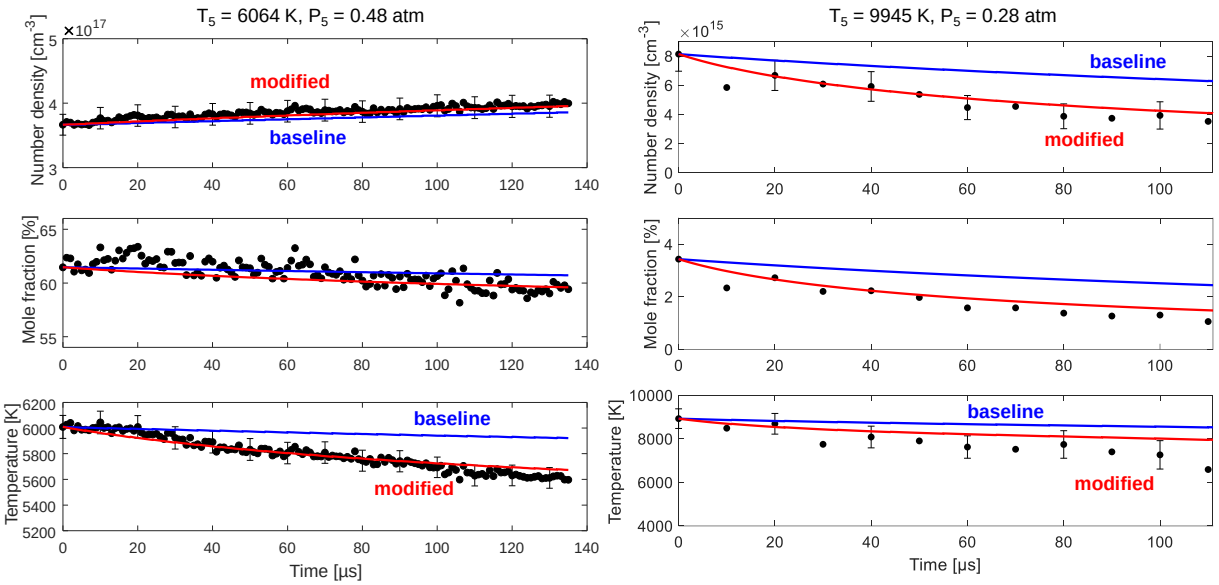

Fig. 4 Typical comparison of the CO dissociation with the baseline mechanism and the modified mechanism. (Left) Low-temperature case for CO:Ar = 60:40. (Right) High-temperature case for CO:Ar = 97:3. The spectra acquired at 1 MHz are time-averaged on a 100-kHz time base (see text).

For low-temperature cases ($T_5 < 6000$ K) and at nearly constant pressure, the drop in temperature induces an overall number density increase, which can virtually compensate for the chemical CO depletion. This effect is responsible for the effective increase of N_{CO} in Fig. 4 (left) and is taken into account in the rate optimization. For high-temperature cases ($T_5 > 6000$ K), this effect is still present but less pronounced compared to the temperature drop due to CO dissociation.

As shown in Fig. 4, the baseline mechanism under-predicts the reactivity of the mixture: the simulated X_{CO} is always higher than the experimental one. As a consequence of underpredicting the endothermic dissociation, the temperature simulated via the baseline mechanism is also higher than the experimental one. A fitting loop is implemented to reduce the residual, R, between the simulated and the experimental results for both the number density and temperature parameters, see Eq. 3 where R is the residual, N_{Run}, the total number of experiments, M, the total number of time-resolved data points per shock, N_{sim} (or T_{sim}), the simulated number density (or temperature), and N_{exp} (or T_{exp}), the experimental number density (or temperature).

$$R = \frac{1}{N_{Run}} \sum_{\text{Run}} \left[\frac{1}{M} \sqrt{\sum_{i}^{M} \left(\frac{N_{\text{CO,sim}}(i) - N_{\text{CO,exp}}(i)}{\Delta N_{\text{CO,exp}}(i)} \right)^2} + \frac{1}{M} \sqrt{\sum_{i}^{M} \left(\frac{T_{\text{sim}}(i) - T_{\text{exp}}(i)}{\Delta T_{\text{exp}}(i)} \right)^2} \right] \tag{3}$$

The norm L2 shown in Eq. 3 is normalized by the experimental time-resolved uncertainty, $\Delta N_{\text{CO,exp}}$ and $\Delta T_{\text{CO,exp}}$. This formulation has the advantage of (i) balancing the optimization using number density and temperature equally and (ii) applying more weight to the low-uncertainty measurements. The optimization is run on 40 shocks with conditions spanning across $P_5 = 0.26 - 4.1$ atm, $T_5 = 4650 - 11{,}150$ K, and $X_{CO} = 3 - 60\%$. During the loop, the pre-exponential

factor and the temperature coefficient of (R1) and (R2) are floated, whereas the activation energy is held constant at 129,000 K (= 11.1 eV) [4, 6]. Note that we kept this established value, although more recent calculations have indicated that the actual dissociation temperature is 130,462 K [28]. Slightly anticipating the description of Section IV, the simulation using the modified rates (i.e. the modified mechanism) is also shown in Fig. 4 and follows the trends of temperature and number density evolution more closely than the baseline mechanism.

IV. Results and discussion

In this section, the findings of the experimental campaign and the rate coefficient optimization are discussed and compared to the available rates in the literature. First, in Sec. IV.A, the rate coefficients measured experimentally in the literature are reviewed. Then, in Sec. IV.B, recent calculations of the CO dissociation and O exchange rate coefficients are presented. Finally, in Sec. IV.C, our modified rate coefficients are compared to the aforementioned rate parameters.

A. Previous experimental work on CO dissociation

Carbon monoxide dissociation has been the subject of numerous works summarized here in the following paragraph and Table 1. For context, we repeat here the main reactions of interest, (R1) & (R2), relevant to our experiments performed with CO diluted in Ar.

$$CO + CO \longleftrightarrow C + O + CO \tag{R1}$$

$$CO + Ar \longleftrightarrow C + O + Ar \tag{R2}$$

In 1964, Davies monitored CO dissociation in Ar using the CO fundamental band emission at 4.65 µm, assumed to be proportional to CO concentration [29, 30]. The UV electronic system of CO at 643 nm was also measured and showed similar decay rates. Their data were refitted by Dickerman [30] who provided coefficients for the entire temperature range studied by Davies. Several studies followed based on optical emission spectroscopy (OES) techniques. Presley, Chackerian, and Watson [31] measured the decay of CO overtone emission ($\Delta v = -2$) to estimate the CO+CO dissociation rate coefficient. Their measurements required taking into account the temperature evolution, which was performed a few years later by Chackerian [32]. The rate coefficient found in [32] was approximately 10 times higher than in [31]. In 1969, Fairbairn [33] was the first to propose that CO* and C_2 could be potential intermediates of CO dissociation. In mixtures of CO and O_2 diluted in Ar, Appleton et al. [34] used the absorption of the 117.6-nm electronic transition of CO to track its number density. They found an apparent CO dissociation energy of 8–8.5 eV, in line with what Davies and Presley found previously and suggesting that intermediates could lower the activation energy of (R1) and (R2). They also proposed a 4-step dissociation mechanism that could qualitatively explain the results available at that time. Hanson [35] used pressure measurements in pure CO to complement the available dissociation rate coefficients obtained with optical diagnostics. He found an effective CO dissociation rate with a coefficient not

Authors (year)	CO+M	Diagnostic	Wavelength	Incubation	Shock-tube id.	Ref.
Davies (1964)	Ar	OES: CO	643 nm, 4.6 µm	no		[29, 30]
Presley et al. (1966)	CO	OES: CO	2–4 µm	no	30.48 cm	[31]
Fairbairn (1969)	Ar	OES: CO	4.6 µm	yes	3.81 cm	[33, 37]
Appleton et al. (1970)	Ar, O	Absorption: CO	117 nm	yes	7.6 cm	[34]
Chackerian (1971)	CO	OES: CO	2.3–3.6 & 4.6 µm	/	30.48 cm	[32]
Hanson (1974)	CO	Pressure	/	no	7.6 cm	[35]
Mick et al. (1993)	Ar	ARAS: O, C	UV	yes	7.9 cm	[36]
Johnston and Brandis (2014)	CO, Ar[(a)]	OES: CN, CO	UV	no	10.16 cm	[6]
Cruden et al. (2018)	CO[(b)]	OES: C_2, CO	Vis, VUV & IR	no	10.16 cm	[7]
This work	CO, Ar	LAS: CO	5 µm	no	10.32 cm	

[(a)] Experiments performed in synthetic Mars atmosphere with traces of Ar. During the rate coefficient optimization, the ratio of Ar+CO and CO+CO rate coefficients was kept equal to 10 following the work of Park et al. [4].
[(b)] Cruden et al. did not propose new rates but gave a critical review of the relevance of the available ones based on new experiments.

Table 1 List of experimental CO dissociation experiments performed in shock tubes. Only the dissociative colliders relevant to the present study (M = CO, Ar or O) are shown even if other particles were considered in the references. OES: optical emission spectroscopy, ARAS: atomic resonance absorption spectroscopy, LAS: laser absorption spectroscopy, id.: internal diameter

compatible with collision theory, see [31], but able to describe his experiments from 5600 to 12,000 K. In 1993, Mick et al. [36] measured O and C number density via atomic resonance absorption spectroscopy (ARAS). Thanks to the high dilution of their experiments ($X_{CO} < 1\%$), the rate of O and C formation was only sensitive to the Ar+CO dissociation, (R2). They also showed that in highly diluted cases, the VT relaxation had no significant impact on the kinetics. Based on the aforementioned works and others, Park et al. [4] proposed a kinetic mechanism to describe shock-heated CO_2-N_2 mixtures, which is still commonly used as a reference.

After a pause of nearly 20 years, a renewed interest in CO dissociation arose because the Park mechanism did not agree with measurements representative of high-speed entry on Venus and Mars [5]. Using the electric arc shock tube (EAST) of NASA Ames [1, 5] with mixtures representative of Mars and Venus, Johnston and Brandis [6] adjusted the rate coefficients of several reactions from the Park mechanism and found better agreement with their new set of data. Motivated by *ab initio* rate coefficients calculated by Schwenke et al. [26] (described later), new experiments were performed on the same shock tube, EAST, by Cruden et al. [7] using pure CO. The measurements of Cruden et al. showed that an electronically excited state of CO is likely an intermediate of dissociation. The radiance measured at multiple wavelengths was found to be in agreement with the model when including the Johnston and Brandis CO dissociation rate above 6.6 km/s (i.e. for high-temperature cases), but was in better agreement with Hanson's rate for shock speeds below 6.6 km/s (i.e. for low-temperature cases). To our knowledge, this is the last shock-tube study only devoted to CO dissociation. In 2023, in a work mainly focused on ablating materials, Cruden et al. [38] proposed a new rate of CO dissociation based upon that of Schwenke et al. [26], but modified to account for electronic excitation as discussed in [7]. The corresponding temperature range is not explicitly stated in [38] and is estimated in Fig. 5.

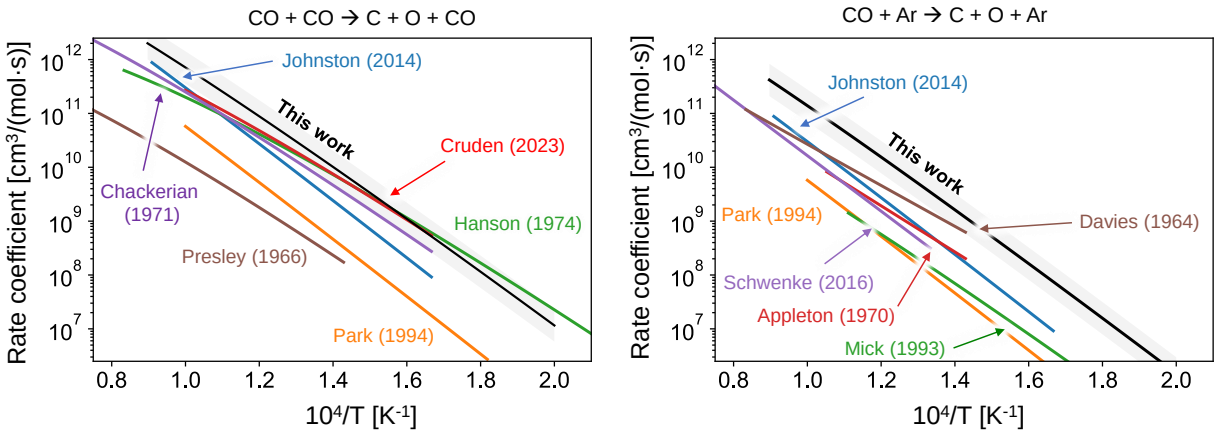

Fig. 5 Comparison of our proposed rate coefficients (in black) with literature sources for (R1) and (R2). A shaded area is used to represent an uncertainty factor of 2.

As shown in Fig. 5, the Cruden (2023) rate coefficient is very close to that of Hanson [35]. All the rate coefficients discussed above are plotted in Fig. 5 and their numerical values are given in Table 3.

It should be noted that three groups observed so-called "induction time", denoting a delay between the shock wave and the onset of CO dissociation, see Table 1. Fairbairn was the first one to report this effect in [37] and later described the phenomenon thoroughly in [33]. Appleton et al. [34] observed induction times of ~10 µs at 8000 K which were in good agreement with the delays reported by Fairbairn. Finally, Mick et al. [36] also observed induction times but an order of magnitude shorter than those of Fairbairn and Appleton. Although this feature was observed with three different optical techniques, it could not be reproduced in the other works reported in Table 1. This effect cannot be explained by a vibrational ladder because VT relaxation is typically 10 to 100 times faster. In our measurements, no induction delay was observed (see also Figure 10 & 11 in our previous work [14]) and for the remainder of this article, the induction period will not be considered.

B. Previous numerical work on CO dissociation and CO+O exchange rate

Simulations of CO+M collisions have been performed to describe (i) rotational and vibrational relaxation, (ii) atom exchange, and (iii) CO dissociation - see a summary in Table 2. Fujita [25] calculated *ab initio* the potential energy surfaces of CO + O. From this, he showed that the rotational-translational (RT) and VT relaxation rates are almost equal above 4000 K and proposed a correction to the CO+O VT coefficients of Park [4]. The rate of CO+O dissociation, (R5), calculated by Fujita is approximately equal to the rate of CO+Ar dissociation measured by Mick et al. [36].

$$\mathrm{CO + O \longleftrightarrow C + O + O} \tag{R5}$$

Authors (year)	CO+M	Method	Ref.
Fujita (2008)	O *diss.*, O *exc.*	QCT	[25]
Schwenke et al. (2016)	O *diss.*, O *exc.*, Ar	QCT	[26]
Venturi & Panesi (2018)	O *diss.*	CG-QCT	[27]

Table 2 List of numerical studies relevant for the kinetics of CO dissociation. QCT: quasi-classical trajectory, CG-QCT: coarse-grain QCT.

Thus, Fujita admitted that their calculation could require some refinement because O collisions are typically more reactive than Ar collisions. Nevertheless, they showed that, below 40,000 K, the rate of CO+O exchange, (R3), is faster than CO+O dissociation, (R5). Later, Schwenke et al. [26] calculated new *ab initio* electronic potentials from which they derived CO+Ar dissociation, CO+O dissociation, and CO+O exchange rate coefficients. They also showed that CO+O exchange rate coefficient is higher than that of CO+O dissociation but for temperatures below 16,000 K. In consequence, in the presence of O atoms, the dissociation of CO could be dominated by the exchange of an O atom, (R3), followed by the dissociation of O_2, (R4).

$$CO + O \leftrightarrow O_2 + C \tag{R3}$$

$$O_2 + M \leftrightarrow O + O + M \tag{R4}$$

The impact of these findings could be important for Mars and Venus entry predictions. Indeed, during Mars and Venus entry at 5–8 km/s, the mixture is mostly composed of CO and O due to fast CO_2 dissociation*. Using the electronic potentials calculated by Schwenke et al., Venturi and Panesi [27] showed that in a mixture of CO:O = 50:50, the inclusion of CO+O exchange leads to an acceleration of CO dissociation. As of today, the mechanisms of Johnston and Brandis [6] and Cruden et al. [7] reproduce well the shock-tube data [39, 40] and the measurements performed on MEDLI2 [41, 42]. The rates calculated by Schwenke et al. were found to be coherent with the *experimental data* of Johnston and Brandis, see [43], but were in less good agreement than the *kinetic mechanism* of Johnston and Brandis which was optimized for their data.

In this work, the CO+O exchange rate is taken from Park [4] (as done in [6, 7]). As described in the previous paragraph, this rate could be improved. However, in Section III.B, the sensitivity analysis showed that (R3) and (R4) do not influence CO number density in our case, see Fig. 3, because our study is performed for CO diluted in Ar. We note however that in pure CO_2, the impact of (R3) and (R4) would be higher, but this study is left for future work.

*Estimations based on those presented by Schwenke et al. [26] for entry speeds of 5–8 km/s.

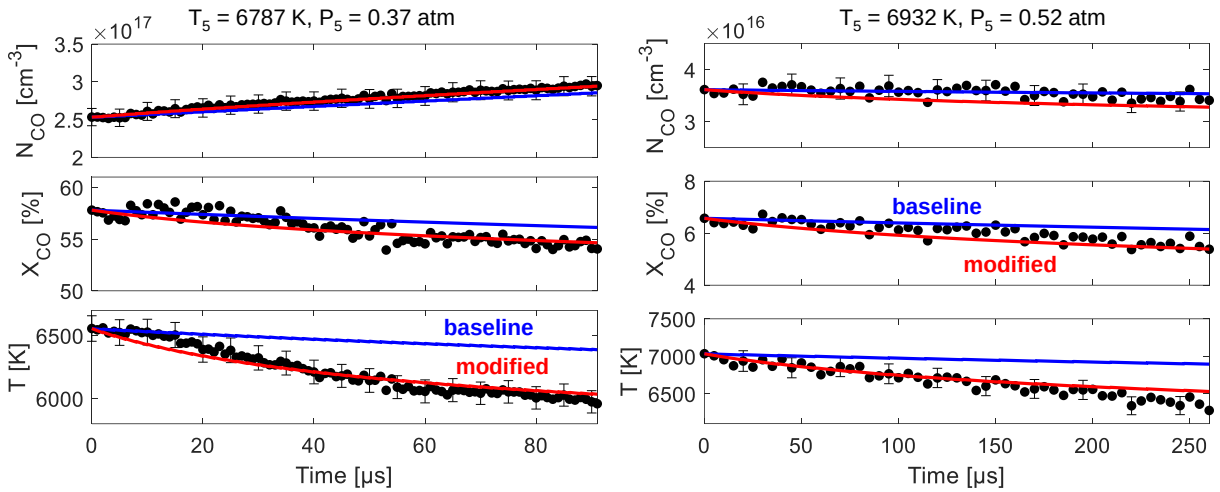

Fig. 6 Effect of the pressure and the initial CO mole fraction on the optimization.

C. Comparison of the present rate coefficient with the literature

The modified rate coefficients calculated via our optimization procedure are shown in Fig. 5 and given here:

$$k_{\text{diss, CO}} = 1.8 \times 10^{28} \cdot T^{-2.7} \exp\left(\frac{-129,000\ \text{K}}{T}\right)\ [\text{cm}^3/(\text{mol} \cdot \text{s})] \tag{4}$$

$$k_{\text{diss, Ar}} = 1.5 \times 10^{25} \cdot T^{-2.1} \exp\left(\frac{-129,000\ [\text{K}]}{T}\right)\ [\text{cm}^3/(\text{mol} \cdot \text{s})] \tag{5}$$

As mentioned before, the optimization was run on 40 shocks with conditions spanning across $P_5 = 0.26 - 4.1$ atm, $T_5 = 4650 - 11{,}150$ K, and $X_{\text{CO}} = 3 - 60\%$. The improvement of the agreement between the simulated and experimental thermo-chemical conditions was already presented in Fig. 4. The effect of pressure is presented in Fig. 6 with two shocks ran near 6800 K at 0.37 atm and 0.52 atm. This figure is also an opportunity to assess the impact of the initial mole fraction from 6% to 58%. The increase in pressure and mole fraction does not show an impact on the quality of the optimization.

The effect of temperature is illustrated in Fig. 6 where the initial mole fraction of CO is always near 10% and T_5 is increased from Fig. 7 a) to f). At this mole fraction, the sensitivity to CO+Ar and CO+CO dissociation is of the same order of magnitude.

Near 1 atm and 5300 K in Fig. 7 a), the mole fraction is found to be constant on a 500-µs scale because the dissociation of CO is not active at this temperature and in this time range. The slight increase in number density and temperature is due to an isentropic compression behind the shock wave which is included in the kinetic simulation. The agreement between the simulation and the measurements in this example demonstrates that the shock non-ideal effects are well-accounted for in the 0D solver. When dissociation is noticeable, the modified mechanism performs better than the baseline. We remark that the temperature drop is a better indicator of CO dissociation than the number density

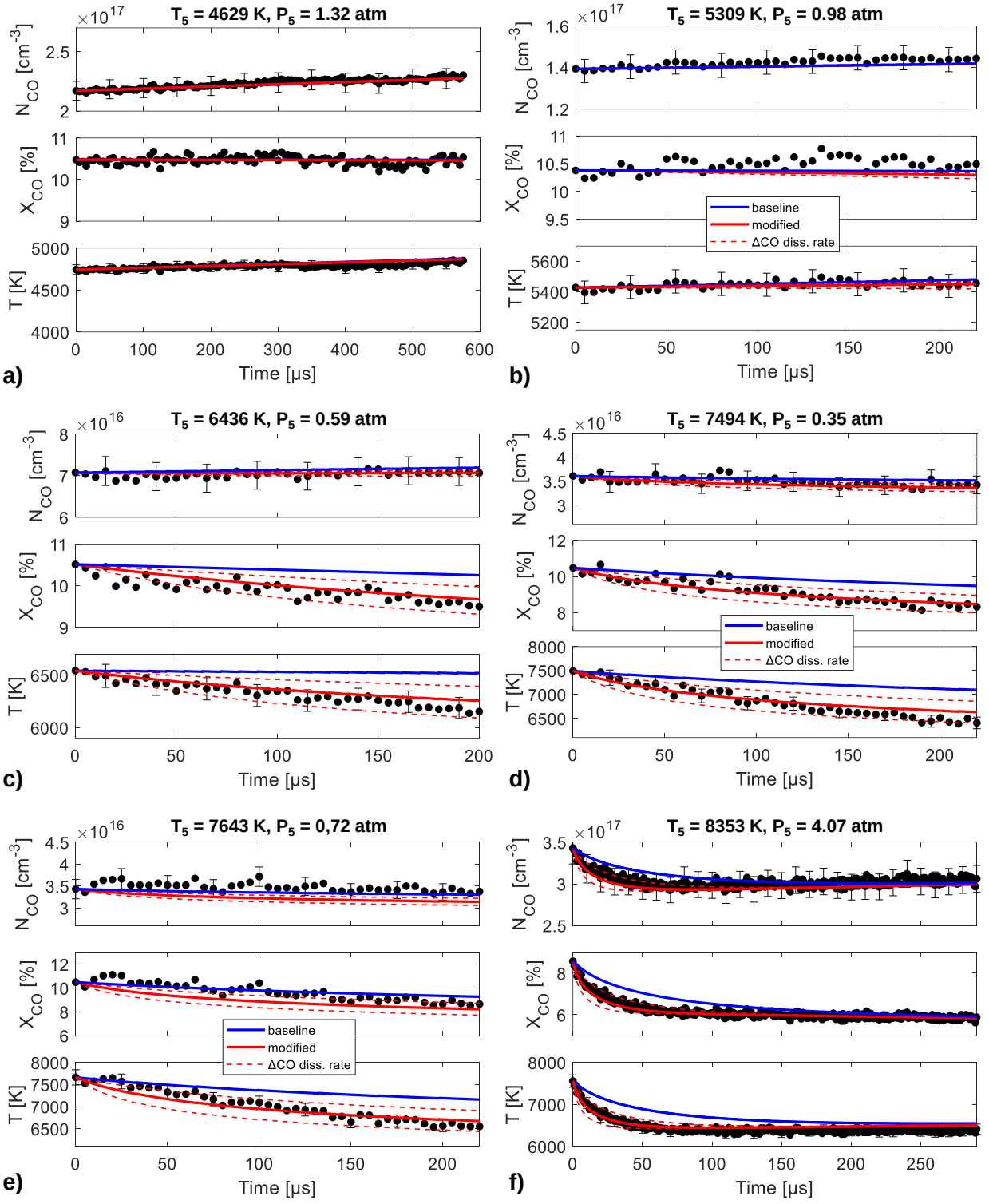

Fig. 7 Comparison of the measured number density, mole fraction, and temperature with the baseline and modified mechanisms from T_5 = 5309 K to T_5 = 8353 K. Simulation results with a variation of the CO+CO and CO+Ar dissociation rates by a factor of two in the modified mechanism are also shown for reference (dashed red lines).

drop. For instance, in Fig. 7 c), the precision of the temperature measurement ($\frac{\Delta T}{T}$ = 1.6% ~ 100 K) is enough to notice i) the 400-K drop in the experimental data points and ii) the difference between the two mechanisms. However, it is difficult to measure the number density drop nor differentiate the two mechanisms ($\frac{\Delta n_{CO}}{n_{CO}}$ = 4.6%). In Fig. 7 f), the start temperature and number density correspond to the first available measurement behind the shock bifurcation.

Using a subset of the 40 shocks and not considering the measurement uncertainties, the result of the optimization varied typically within ± 10% for the pre-exponential factor and within ± 0.1 for the exponent. As shown in Fig. 5, the rate coefficient of CO+CO, (R1), is above the coefficient of Park by a factor of 10. This difference is expected since, in CO_2 atmospheres, the Park mechanism overpredicted the CO emission because of a too-low dissociation rate [6]. Our modified rate coefficient favors the results of Johnston and Brandis [6] at high temperatures and that of Hanson [35] at low temperatures, which is in complete agreement with the findings of Cruden et al. [7]. We also note that our rate coefficient is in close agreement with that of Chackerian [32]. As such, the rate coefficient found in the present work is expected to reasonably match the radiation measurements of [7].

As shown in Fig. 5, our rate coefficient of CO+Ar is notably higher than those measured previously. The difference is within a factor of 30 across all the temperatures when compared to the work of Mick et al., Davies, and Appleton et al. Some of these previously published rate coefficients are closer than others. Notably, at 7000 K, our rate coefficient for CO+Ar is within a factor of two compared to the rate of Davies [29]. We also note that our proposed rate coefficient of CO+Ar, (R2), is approximately five times higher than that of Johnston and Brandis [6], which is at the edge of their claimed uncertainty. The modified kinetic mechanism where these new rate coefficients are included is given in the supplementary material (.YAML file).

Experimental kinetic rates are regularly compared with collision theory for dissociation, e.g. [31, 35]. The theory of collisions for dissociation reactions is detailed in Chap. VII of [44]. According to [44], the rate coefficient of dissociation can be written $k_{\text{diss}} = AT^{\eta} \exp(-\theta/T)$ where θ = 129,000 K is the activation energy of CO dissociation. The factor η must be between -3.5 and -1.5 for molecule-molecule collisions, and between -1.5 and -0.5 for atom-molecule collisions. Our CO+CO coefficient is in line with these ranges although the CO+Ar coefficient is not. However, deviations from collision theory have been noted previously for CO dissociation. For instance, the value of η proposed by Hanson [35] does not agree with the collision theory but performs very well in relatively low-temperature experiments of [7]. Similarly, the value of η proposed by Presley et al. [31] agrees by construction with collision theory but is significantly different from all the experimental rate coefficients of the literature, see Fig. 5. Therefore, we will simply note that our temperature exponent of CO+Ar is higher than that of CO+CO (-2.7 < -2.1), which agrees with the ordering predicted by the collision theory of dissociation.

The ratio of rate coefficients is also commonly employed in the literature for comparisons [26] and is revisited here. As shown in Fig. 8, the ratio of our rate coefficients $k_{\text{diss, CO}}/k_{\text{diss, Ar}}$ is found to be equal to 6.0 on average. This ratio is close to the value of 10 chosen by Park et al. [4] and later reused by Johnston and Brandis [6]. At that time, Park et al.

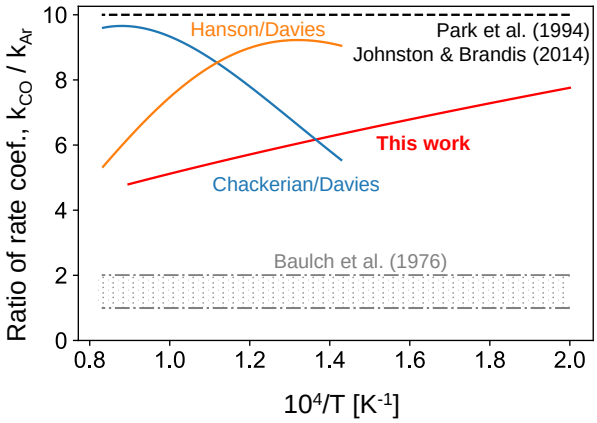

Fig. 8 Comparison of the relative dissociation efficiencies of CO and Ar found in this work (in red) and the one assumed constant in the mechanism of Park et al. [4] and Johnston and Brandis [6] (in dashed black). The relative dissociation efficiency is also shown by taking the rate coefficients of other authors who published before 1994 [29, 32, 35] and the recommendations of Baulch et al. [45].

used a ratio of 10 because this ratio was also employed for CO_2 dissociation by Ar and molecules. We note however that the compendium of Baulch et al. [45] suggests rather to use a ratio of 1 – 2 based on the data of Appleton et al. [34] and Presley et al. [31]. Using the data of Hanson and Davies in Fig. 8 indicates that a ratio of 10 is a plausible approximation. However, using the data of Chackerian and Davies provides an average ratio between 6 and 8. The rate ratio derived from this work spans between 5 and 8, which is very similar to the ratio of Chackerian/Davies but over a larger range. Overall, the graphical comparison in Fig. 8 indicates that the ratio of the two rate coefficients determined in this work is quite reasonable.

D. Uncertainty estimation

The rigorous evaluation of the uncertainty in measuring a rate coefficient is a difficult task. Among the previous studies that measured the rate coefficient of CO+Ar and CO+CO, only Johnston and Brandis [6] performed an estimation of the uncertainty. In this present work, we followed their procedure and modified the optimized rate coefficients at multiple temperatures to find the variation that most closely matched the bounds of the experimental number density and temperature uncertainties. In Fig. 7, the variation of the simulated T, N_{CO}, and X_{CO} is presented when the rate coefficients of (R1) and (R2) are varied by a factor of two. This graphical representation demonstrates that an uncertainty of factor two in the rate coefficients satisfactorily agrees with the experimental data. This estimated uncertainty in our rate coefficient determination is also illustrated by the grey shaded area in Fig. 5.

V. Conclusions

High-speed mid-infrared laser absorption spectroscopy was employed to measure CO number density and temperature in shock-heated mixtures of CO and Ar at conditions relevant to Mars and Venus entry. These measurements were shown to be a sensitive and quantitative method for determining the CO rate of dissociation due to collisions with M = Ar or CO in CO + M $\rightarrow$ C + O + M. The influence of O atom exchange is found to be negligible in our conditions. The rate coefficient optimization is found to be strongly constrained by the temperature measurement. The CO+Ar dissociation rate coefficients measured in this work are relatively higher than previous measurements in the literature but remain within the same order of magnitude as reported in previous studies. The CO+CO dissociation rate coefficient of this study is in very close agreement with Johnston and Brandis [6] near 11,150 K and with Hanson [35] near 4,650 K, which is consistent with the recent emission measurements performed by Cruden et al. [7] in shock-heated undiluted CO. The ratio of our rate coefficients $k_{\text{diss, CO}}/k_{\text{diss, Ar}}$ is found to be a weak function of temperature and equal to approximately 6 on average. This work provides new rate parameters that may ultimately improve the modeling of the thermochemical state evolution during Mars and Venus entry. Future analogous work focused on O_2 and CO mixtures, where the CO + O dissociation would dominate, is expected to provide further insight into such entry thermophysical kinetics.

Appendix: List of the available rate coefficients of CO dissociation in Ar and CO

The rate coefficients in Table 3 are given for an Arrhenius form: $k = AT^n \exp(T/E_a)$. Some authors attempted to fit their data with a combination of fixed and floated parameters (mainly the activation energy, E_a, and the temperature exponent, n). Only one formulation is provided here because they all provide effectively the same value, but the interested reader is invited to consult Table 1 of [26].

Acknowledgment

This work was sponsored by NASA's Space Technology Research Grants Program via an Early Career Faculty award 80NSSC21K0066. The authors thank Anil Nair and Nick Kuenning for their help in the shock tube operation and for insightful discussions about these experiments. The authors also thank Brett Cruden, Megan Macdonald, and Augustin Tibère-Inglesse at NASA Ames for their feedback about this work.

References

[1] Cruden, B. A., Prabhu, D., and Martinez, R., "Absolute Radiation Measurement in Venus and Mars Entry Conditions," *Journal of Spacecraft and Rockets*, Vol. 49, No. 6, 2012, pp. 1069–1079. https://doi.org/10.2514/1.A32204, URL https://arc.aiaa.org/doi/10.2514/1.A32204.

[2] McGuire, S. D., Tibère-Inglesse, A. C., and Laux, C. O., "Infrared spectroscopic measurements of carbon monoxide

Authors (year)	Range [K]	M	A [cm^3/(mol·s)]	n	E_a [K]	Ref.
Davies (1964)	7,000–9,500	Ar	3.49×10^{12}	0.5	92,830	[29, 30]
	9,000–12,000		1.57×10^{11}	0.5	63,820	
	7,000–15,000		1.14×10^{12}	0.5	83550	
Presley et al. (1966)	7,000–15,000	CO	5×10^{29}	-3.5	129,000	[31]
Appleton et al. (1970)	8,000–15,000	Ar	1.69×10^{27}	-2.86	129,000	[34]
Chackerian (1971)	6,000–16,000	CO	1.0×10^{31}	-3.5	129,000	[32]
		Ar	1.0×10^{31}	-3.5	129,000	
Hanson (1974)	5,600–12,000	CO	8.0×10^{38}	-5.5	129,000	[35]
Mick et al. (1993)	5,500–9000	Ar	4.3×10^{27}	-3.1	129,000	[36]
Park et al. (1994)	N.P.[(a)]	CO	2.3×10^{20}	-1.0	129,000	[4]
		Ar	2.3×10^{19}	-1.0	129,000	
Johnston and Brandis (2014)	N.P.[(a)]	CO	1.2×10^{21}	-1.0	129,000	[6]
		Ar[(b)]	1.2×10^{20}	-1.0	129,000	
Schwenke et al. (2016)	7,500–20,000	Ar	2.35×10^{15}	0	118712.6	[26]
Cruden et al. (2023)	N.P.[(a)]	M[(c)]	8.36×10^{35}	-4.72	129,230	[38]
This work	4,650–11,150	CO	1.9×10^{28}	-2.7	129,000	
		Ar	1.4×10^{25}	-2.1	129,000	

[(a)] Not Provided: The temperature range to employ this rate coefficient was not specified by the authors.
[(b)] Experiments performed in synthetic Mars atmosphere with traces of Ar. During the rate coefficient optimization, the ratio of Ar+CO and CO+CO rate coefficients was kept equal to 10 following the work of Park et al. [4].
[(c)] The efficiency of the reaction depending on the collider (M = Ar, CO ...) is not specified.

Table 3 CO dissociation rate coefficients for CO+CO (R1) and CO+Ar (R2)

within a high temperature ablative boundary layer," *Journal of Physics D: Applied Physics*, Vol. 49, No. 48, 2016. https://doi.org/10.1088/0022-3727/49/48/485502.

[3] Lewis, S. W., James, C. M., Morgan, R. G., McIntyre, T. J., Alba, C. R., and Greendyke, R. B., "Carbon ablative shock-layer radiation with high surface temperatures," *Journal of Thermophysics and Heat Transfer*, Vol. 31, No. 1, 2017, pp. 193–204. https://doi.org/10.2514/1.T4902.

[4] Park, C., Howe, J. T., Jaffe, R. L., and Candler, G. V., "Review of chemical-kinetic problems of future NASA missions, II: Mars entries," *Journal of Thermophysics and Heat Transfer*, Vol. 8, No. 1, 1994, pp. 9–23. https://doi.org/10.2514/3.496.

[5] Brandis, A. M., Johnston, C. O., and Cruden, B. A., "Investigation of non-equilibrium radiation for earth entry," *46th AIAA Thermophysics Conference*, , No. January, 2016, pp. 1–36.

[6] Johnston, C., and Brandis, A., "Modeling of nonequilibrium CO Fourth-Positive and CN Violet emission in CO 2 –N 2 gases," *Journal of Quantitative Spectroscopy and Radiative Transfer*, Vol. 149, 2014, pp. 303–317. https://doi.org/10.1016/j.jqsrt.2014.08.025, URL http://dx.doi.org/10.1016/j.jqsrt.2014.08.025https://linkinghub.elsevier.com/retrieve/pii/S0022407314003690.

[7] Cruden, B. A., Brandis, A. M., and Macdonald, M. E., "Characterization of CO thermochemistry in incident shockwaves," *2018 Joint Thermophysics and Heat Transfer Conference*, 2018, pp. 1–22. https://doi.org/10.2514/6.2018-3768.

[8] MacDonald, M. E., and Cruden, B. A., "A tunable laser absorption diagnostic for measurements of CO in shock-heated gases," *46th AIAA Thermophysics Conference*, , No. June, 2016, pp. 1–12. https://doi.org/10.2514/6.2016-3694.

[9] Macdonald, M. E., Brandis, A. M., and Cruden, B. A., "Post-Shock temperature and CO Number density measurements in CO and CO2," *47th AIAA Thermophysics Conference, 2017*, , No. June, 2017, pp. 1–18. https://doi.org/10.2514/6.2017-4342.

[10] MacDonald, M. E., Brandis, A. M., and Cruden, B. A., "Temperature and CO Number Density Measurements in Shocked CO and CO2 via Tunable Diode Laser Absorption Spectroscopy," *2018 Joint Thermophysics and Heat Transfer Conference*, American Institute of Aeronautics and Astronautics, Reston, Virginia, 2018, pp. 1–23. https://doi.org/10.2514/6.2018-4067, URL https://arc.aiaa.org/doi/10.2514/6.2018-4067.

[11] Jelloian, C. C., Bendana, F. A., Wei, C., Spearrin, R. M., and Macdonald, M. E., "Simultaneous vibrational, rotational, and translational thermometry based on laser absorption of co in shock-induced non-equilibrium," *AIAA Scitech 2021 Forum*, American Institute of Aeronautics and Astronautics, Reston, Virginia, 2021, pp. 2021–0448. https://doi.org/10.2514/6.2021-0448.c1, URL https://arc.aiaa.org/doi/10.2514/6.2021-0448.

[12] Lin, X., Chen, L. Z., Li, J. P., Li, F., and Yu, X. L., "Experimental and Numerical Study of Carbon-Dioxide Dissociation for Mars Atmospheric Entry," *Journal of Thermophysics and Heat Transfer*, Vol. 32, No. 2, 2018, pp. 503–513. https://doi.org/10.2514/1.T5152, URL https://arc.aiaa.org/doi/10.2514/1.T5152.

[13] Jelloian, C. C., Bendana, F. A., Wei, C., Spearrin, R. M., and MacDonald, M. E., "Nonequilibrium Vibrational, Rotational, and Translational Thermometry via Megahertz Laser Absorption of CO," *Journal of Thermophysics and Heat Transfer*, Vol. 36, No. 2, 2022, pp. 266–275. https://doi.org/10.2514/1.T6376, URL https://arc.aiaa.org/doi/10.2514/1.T6376.

[14] Minesi, N. Q., Richmond, M. O., Jelloian, C. C., Kuenning, N. M., Nair, A. P., and Spearrin, R. M., "Multi-line Boltzmann regression for near-electronvolt temperature and CO sensing via MHz-rate infrared laser absorption spectroscopy," *Applied Physics B: Lasers and Optics*, Vol. 128, No. 12, 2022. https://doi.org/10.1007/s00340-022-07931-7, URL https://link.springer.com/10.1007/s00340-022-07931-7.

[15] Bendana, F. A., Lee, D. D., Spearrin, R. M., Schumaker, S. A., and Danczyk, S. A., "Infrared laser absorption thermometry and CO sensing in high-pressure rocket combustion flows from 25 to 105 bar," *AIAA Scitech 2019 Forum*, American Institute of Aeronautics and Astronautics, 2019. https://doi.org/10.2514/6.2019-1610.

[16] Pineda, D. I., Bendana, F. A., Schwarm, K. K., and Spearrin, R. M., "Multi-isotopologue laser absorption spectroscopy of carbon monoxide for high-temperature chemical kinetic studies of fuel mixtures," *Combustion and Flame*, Vol. 207, 2019, pp. 379–390. https://doi.org/10.1016/j.combustflame.2019.05.030, URL https://linkinghub.elsevier.com/retrieve/pii/S0010218019302433.

[17] Nair, A., Lee, D., Pineda, D., Kriesel, J., Hargus, W., Bennewitz, J., Danczyk, S., and Spearrin, R., "MHz laser absorption spectroscopy via diplexed RF modulation for pressure, temperature, and species in rotating detonation rocket flows," *Applied Physics B*, Vol. 126, No. 8, 2020, p. 138. https://doi.org/10.1007/s00340-020-07483-8, URL https://link.springer.com/10.1007/s00340-020-07483-8.

[18] Nair, A. P., Minesi, N. Q., Jelloian, C., Kuenning, N. M., and Spearrin, R. M., "RF-waveform optimization for MHz-rate DFB laser absorption spectroscopy in dynamic combustion environments," *AIAA Science and Technology Forum and Exposition, AIAA SciTech Forum 2022*, 2022, pp. 1–13. https://doi.org/10.2514/6.2022-2373.

[19] Gamache, R. R., Vispoel, B., Rey, M., Nikitin, A., Tyuterev, V., Egorov, O., Gordon, I. E., and Boudon, V., "Total internal partition sums for the HITRAN2020 database," *Journal of Quantitative Spectroscopy and Radiative Transfer*, Vol. 271, 2021, p. 107713. https://doi.org/10.1016/j.jqsrt.2021.107713, URL https://doi.org/10.1016/j.jqsrt.2021.107713https://linkinghub.elsevier.com/retrieve/pii/S0022407321002065.

[20] Rothman, L., Gordon, I., Barber, R., Dothe, H., Gamache, R., Goldman, A., Perevalov, V., Tashkun, S., and Tennyson, J., "HITEMP, the High-Temperature Molecular Spectroscopic Database," *Journal of Quantitative Spectroscopy and Radiative Transfer*, Vol. 111, No. 15, 2010, pp. 2139–2150. https://doi.org/10.1016/j.jqsrt.2010.05.001.

[21] Petersen, E. L., and Hanson, R. K., "Nonideal effects behind reflected shock waves in a high-pressure shock tube," *Shock Waves*, Vol. 10, No. 6, 2001, pp. 405–420. https://doi.org/10.1007/PL00004051, URL http://link.springer.com/10.1007/PL00004051.

[22] B. J. McBride, M. J. Zehe, and S. Gordon, "NASA Glenn coefficients for calculating thermodynamic properties of individual species," *John H. Glenn Research Center at Lewis Field*, , No. September, 2002. URL http://gltrs.grc.nasa.gov/GLTRS.

[23] Millikan, R. C., and White, D. R., "Systematics of Vibrational Relaxation," *The Journal of Chemical Physics*, Vol. 39, No. 12, 1963, pp. 3209–3213. https://doi.org/10.1063/1.1734182.

[24] Aliat, A., Chikhaoui, A., and Kustova, E. V., "Nonequilibrium kinetics of a radiative CO flow behind a shock wave," *Physical Review E - Statistical Physics, Plasmas, Fluids, and Related Interdisciplinary Topics*, Vol. 68, No. 5, 2003, pp. 1–11. https://doi.org/10.1103/PhysRevE.68.056306.

[25] Fujita, K., "Vibrational Relaxaion and Dissociation Kinetics of CO by CO-O Collisions," *40th Thermophysics Conference*, American Institute of Aeronautics and Astronautics, Reston, Virigina, 2008, pp. 23–26. https://doi.org/10.2514/6.2008-3919, URL https://arc.aiaa.org/doi/10.2514/6.2008-3919.

[26] David W. Schwenke, Jaffe, R. L., and Chaban, G. M., "Collisional Dissociation of CO: ab initio Potential Energy Surfaces and Quasiclassical Trajectory Rate Coeffcients," 2016.

[27] Venturi, S., and Panesi, M., "Investigating CO Dissociation by means of Coarse Grained Ab-Initio Rate Constants," *2018 AIAA Aerospace Sciences Meeting*, American Institute of Aeronautics and Astronautics, Reston, Virginia, 2018, pp. 1–13. https://doi.org/10.2514/6.2018-1232, URL https://arc.aiaa.org/doi/10.2514/6.2018-1232.

[28] Coxon, J. A., and Hajigeorgiou, P. G., "Direct potential fit analysis of the X 1Σ+ ground state of CO," *The Journal of Chemical Physics*, Vol. 121, No. 7, 2004, pp. 2992–3008. https://doi.org/10.1063/1.1768167, URL https://pubs.aip.org/aip/jcp/article/121/7/2992/464294/Direct-potential-fit-analysis-of-the-X-1-groundhttps://pubs.aip.org/aip/jcp/article/121/7/2992-3008/464294.

[29] Davies, W. O., "Radiative energy transfer on entry into Mars and Venus," Tech. rep., Quarterly Report to NASA, IIT Research Institute, Chicago, IL, 1964.

[30] P. J. Dickerman, "Radiative energy transfer on entry into Mars and Venus - Final report," Tech. rep., NASA-CR-100897, 1969.

[31] Presley, L., Chackerian, J., C., and Watson, R., "The dissociation rate of carbon monoxide between 7,000 deg and 15,000 deg K," *3rd and 4th Aerospace Sciences Meeting*, American Institute of Aeronautics and Astronautics, Reston, Virigina, 1966. https://doi.org/10.2514/6.1966-518, URL https://arc.aiaa.org/doi/10.2514/6.1966-518.

[32] Chackerian, J., C., "The dissociation of shock heated carbon monoxide studied by two wavelength infrared emission," *INTERNATIONAL SHOCK TUBE SYMPOSIUM*, IMPERIAL COLL. OF SCIENCE AND TECHNOLOGY,, London, UK, 1971, p. 40.

[33] Fairbairn, A. R., "The dissociation of carbon monoxide," *Proceedings of the Royal Society of London. A. Mathematical and Physical Sciences*, Vol. 312, No. 1509, 1969, pp. 207–227. https://doi.org/10.1098/rspa.1969.0149, URL https://royalsocietypublishing.org/doi/10.1098/rspa.1969.0149.

[34] Appleton, J. P., Steinberg, M., and Liqtjornik, D. J., "Shock-tube study of carbon monoxide dissociation using vacuum-ultraviolet absorption," *The Journal of Chemical Physics*, Vol. 52, No. 5, 1970, pp. 2205–2221. https://doi.org/10.1063/1.1673286.

[35] Hanson, R. K., "Shock-tube study of carbon monoxide dissociation kinetics," *The Journal of Chemical Physics*, Vol. 4970, No. August 2003, 1974, pp. 4970–4976. https://doi.org/10.1063/1.1681010.

[36] Mick, H. J., Burmeister, M., and Roth, P., "Atomic resonance absorption spectroscopy measurements on high-temperature CO dissociation kinetics," *AIAA Journal*, Vol. 31, No. 4, 1993, pp. 671–676. https://doi.org/10.2514/3.11602.

[37] Fairbairn, A. R., "Presence of an incubation time in the dissociation of CO," *The Journal of Chemical Physics*, Vol. 48, No. 1, 1968, pp. 515–516. https://doi.org/10.1063/1.1667961.

[38] Cruden, B. A., Prabhu, D. K., Borner, A., Meurisse, J., Thornton, J., and Bellas-Chatzigeorgis, G., "Assessment of Fluid Dynamics Boundary Condition in Ablating or Blowing Flows," *AIAA Aviation Conference*, 2023.

[39] Tibère-Inglesse, A. C., Cruden, B. A., Jelloian, C. C., and Spearrin, R. M., "Examination of Mars2020 shock-layer conditions via infrared emission spectroscopy of CO2," *AIAA SciTech Conference*, 2023.

[40] Jelloian, C., Minesi, N., Spearrin, R. M., Tibere-Inglesse, A., MacDonald, M. E., and Cruden, B. A., "Examination of Mars2020 shock-layer conditions via infrared laser absorption spectroscopy of CO 2 and CO," *AIAA SCITECH 2023 Forum*, American Institute of Aeronautics and Astronautics, Reston, Virginia, 2023. https://doi.org/10.2514/6.2023-0959, URL http://arc.aiaa.orghttps://arc.aiaa.org/doi/10.2514/6.2023-0959.

[41] Tang, C. Y., Mahzari, M., Prabhu, D. K., Alpert, H. S., and Cruden, B. A., "MEDLI2: MISP Inferred Aerothermal Environment and Flow Transition Assessment," *AIAA Science and Technology Forum and Exposition, AIAA SciTech Forum 2022*, American Institute of Aeronautics and Astronautics Inc, AIAA, 2022. https://doi.org/10.2514/6.2022-0552.

[42] Miller, R. A., Tang, C. Y., White, T. R., and Cruden, B. A., "MEDLI2: MISP Measured Aftbody Aerothermal Environments," *AIAA SCITECH 2022 Forum*, American Institute of Aeronautics and Astronautics, Reston, Virginia, 2022. https://doi.org/10.2514/6.2022-0551, URL https://arc.aiaa.org/doi/10.2514/6.2022-0551.

[43] Jaffe, R. L., Schwenke, D. W., Chaban, G. M., Prabhu, D. K., Johnston, C. O., and Panesi, M., "On the development of a new nonequilibrium chemistry model for Mars entry," *55th AIAA Aerospace Sciences Meeting*, American Institute of Aeronautics and Astronautics, Reston, Virginia, 2017, pp. 1–23. https://doi.org/10.2514/6.2017-1372, URL https://arc.aiaa.org/doi/10.2514/6.2017-1372.

[44] Vincenti, W. G., and Kruger, C. H., *Introduction to Physical Gas Dynamics*, 2nd ed., John Wiley & Sons, Inc., New York, 1967.

[45] Baulch, D. L., Drysdale, D. D., Duxbury, J., and Grant, S. J., *Evaluated kinetic data for high temperature reactions*, Vol. 3, Butterworths (London), 1976.